

# 1 Pathogenic SNPs Affect Both RNA and DNA G-Quadruplexes' 2 Responses to Ligands

3 Marc-Antoine Turcotte and Jean-Pierre Perreault\*



Cite This: <https://doi.org/10.1021/acscchembio.4c00104>



Read Online

ACCESS |



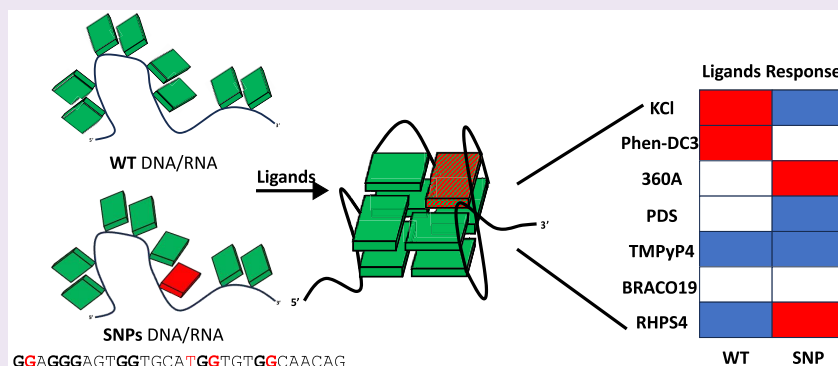
Metrics & More



Article Recommendations



Supporting Information



4 **ABSTRACT:** Single nucleotide polymorphisms (SNPs) are common genetic variations that are present in over 1% of the  
5 population and can significantly modify the structures of both DNA and RNA. G-quadruplex structures (G4) are formed by the  
6 superposition of tetrads of guanines. To date, the impact of SNPs on both G4 ligands' binding efficacies and specificities has not  
7 been investigated. Here, using a bioinformatically predicted G4 and SNPs found in the  $\alpha$ -synuclein gene as a proof-of-concept, it was  
8 demonstrated that SNPs can modulate both DNA and RNA G4s' responses to ligands. Specifically, six widely recognized ligands  
9 (Phen-DC3, PDS, 360A, RHPS4, BRACO19, and TMPyP4) were shown to differentially affect both the structure and the  
10 polymerase stalling of the different SNPs. This work highlights the importance of choosing the appropriate G4 ligand when dealing  
11 with an SNP identified in a G-rich gene.

12 **G**-quadruplexes (G4s) are noncanonical secondary struc-  
13 tures found in both DNA and RNA that are composed of  
14 guanine tetrads.<sup>1</sup> G4s are associated with many cellular  
15 processes including, but not limited to, replication, tran-  
16 scription, and translation.<sup>2</sup> In recent years, thousands of small  
17 molecules have been designed and synthesized to both stabilize  
18 and induce the folding of G4 structures.<sup>3</sup> However, the  
19 efficiency and selectivity of each of these are not only  
20 unpredictable but controlled by many factors, including the  
21 number of G-tetrads, the competition with Watson–Crick base  
22 pairing, and the type of nucleic acid targeted (DNA or  
23 RNA).<sup>4,5</sup> As a consequence, the G-quadruplex/ligand inter-  
24 action can be modulated by modifying only one nucleotide.<sup>6</sup>  
25 Single nucleotide polymorphisms (SNPs) are nucleotide  
26 variations present in more than 1% of the population. Over  
27 600 000 SNPs have been reported in the human genome, with  
28 roughly 30 000 having been associated with various diseases.<sup>7</sup>  
29 Few studies have explored the influence of SNPs on G-  
30 quadruplex formation, and those that did primarily focused on  
31 DNA.<sup>8</sup> For instance, an SNP in the promoter of HSPB2 has  
32 recently been shown to destabilize a G4 and increase the  
33 expression of HSPB2.<sup>9</sup> However, it is important to note that  
34 SNPs can also modulate the folding of RNA G4s and thus

open the way to identifying specific targeting strategies at both  
35 the DNA and the RNA levels. Understanding how these  
36 mutations could affect potential G4 ligand treatments is crucial  
37 for developing targeted therapeutic strategies. Herein, the  
38 ability of SNPs to modulate both DNA and RNA G-  
39 quadruplexes' responses to some of the most often used  
40 ligands was explored.  
41

In order to study the relationship between SNPs, G4s, and  
42 ligands, the sequence of the  $\alpha$ -synuclein gene was used as a  
43 proof-of-concept. The resulting SNCA protein is found at the  
44 neurons' presynaptic terminals and regulates the reserve pool  
45 of synaptic vesicles for neurotransmitter release.<sup>10</sup> However, in  
46 the case of Parkinson's disease, this protein is either  
47 overexpressed or mutated, causing protein aggregation which  
48 leads to, among other things, both proteasomal and  
49

**Received:** February 12, 2024

**Revised:** April 12, 2024

**Accepted:** April 26, 2024

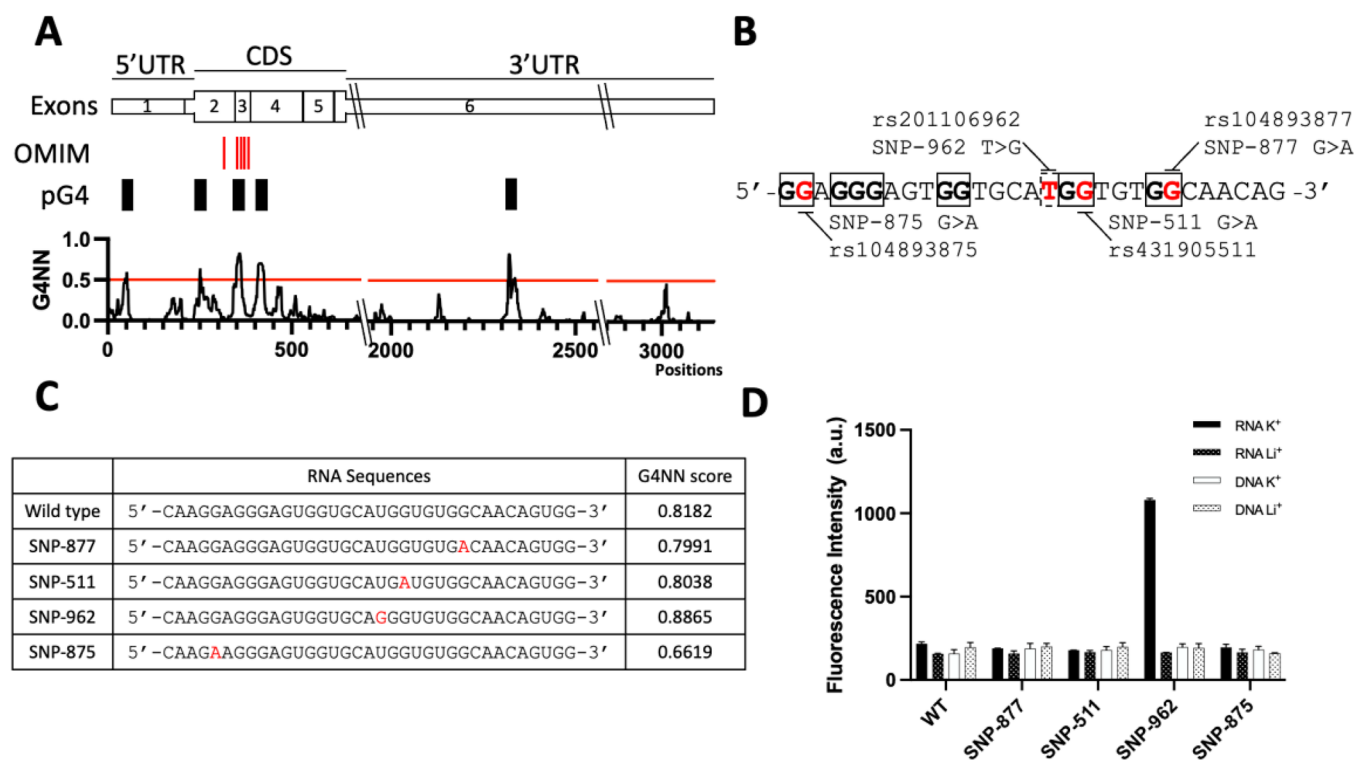


**Figure 1.** Evaluation of pG4 formation in both the  $\alpha$ -synuclein gene and transcript. (A) Representation of the pG4s found in the  $\alpha$ -synuclein transcript and in the OMIM allelic variant phenotype (i.e., the SNPs). The G4NN score for every window along the  $\alpha$ -synuclein transcript is shown. CDS stands for coding sequence and UTR for untranslated region. (B) The four SNPs located in the predicted G4 regions. (C) G4NN score and sequence of the WT and of each SNP. (D) NMM fluorescence at 605 nm of the different RNA and DNA SNP sequences in 20 mM Li-cacodylate buffer in the presence of 100 mM of either potassium chloride or lithium chloride (KCl or LiCl). Results are shown by arbitrary units of fluorescence (a.u.).

50 mitochondrial dysfunction and to an increase in oxidative  
 51 stress.<sup>10</sup> Using the University of California Santa Cruz (USCS)  
 52 database and a neuronal network trained RNA G4 predictor  
 53 (i.e., RNA G4 Screener with the default 0.5 threshold for the  
 54 resulting G4 Neuronal Network (G4NN) score), an RNA  
 55 potential G-quadruplex (pG4) site located in the coding region  
 56 of the  $\alpha$ -synuclein transcript was found to intercept with four  
 57 SNPs known to be associated with both Parkinson's disease  
 58 and with the Lewy body dementia gene (Figure 1A).<sup>7,11</sup> The  
 59 G4NN score, and two other scores of this G4 predictor (cGcG  
 60 and G4 Hunter (G4H)), were also evaluated with different  
 61 sliding window sizes in order to improve the pG4 confidence  
 62 (Figure S1).<sup>12,13</sup> While G4H did not predict the presence of  
 63 any G4s, no matter what the tested window size used was, the  
 64 same G4 "hit" as was found for the G4NN prediction was also  
 65 found with two smaller windows when using cGcG. Based on  
 66 these results, the transcriptomic flanking nucleotides should  
 67 not affect G-quadruplex formation. Of note, smaller windows  
 68 are usually associated with a higher number of hits, but with  
 69 lower precision.<sup>12</sup> Three of these SNPs are guanine to adenine  
 70 (G > A; SNP-877, SNP-511, and SNP875), while one of them,  
 71 SNP-962, is uracil to guanine (U > G; Figure 1B). Despite the  
 72 disruption of the guanine doublet by the mutation to adenine,  
 73 all three SNPs still exhibited a G4NN score higher than the  
 74 threshold (Figure 1C), confirming the prediction of a G4  
 75 despite the nucleotide change (G > A or U > G). As expected,  
 76 the introduction of a guanine (U > G) had a positive effect on  
 77 the score and revealed a high potential for G4 formation as  
 78 compared to the wild type (WT). While the scores remained  
 79 relatively similar (even when using an older predictor, G-rich

sequences (QGRS) Mapper<sup>14</sup>), the presence of the SNPs  
 significantly influenced the number of potential ways that the  
 RNA G4 could fold, ranging from 11 to 53 possibilities.  
 (Supplementary Table 1). Overall, when compared to the WT,  
 SNP-962 seems to be more suitable for G4 formation, while  
 the three other SNPs seem to impair the folding.

Next, the ability of the WT and SNP sequences to fold in  
 G4s *in vitro* was evaluated using the *N*-methylmesoporphyrin  
 IX molecule (NMM), a "turn-on" G4-specific fluorescent  
 ligand.<sup>15</sup> The experiments were performed with both DNA and  
 RNA molecules because SNPs can differently affect their G4  
 formation. An enhanced G4 fluorescence emission at 605 nm  
 was observed exclusively under potassium (K<sup>+</sup>) conditions  
 with SNP-962 in RNA. The differences in the NMM emissions  
 between the lithium (Li<sup>+</sup>) and the K<sup>+</sup> conditions, which were  
 up to 6.5-fold, provided evidence supporting the formation of  
 G4 structures with only SNP-962 in RNA, contradicting the  
 predictions made by the G4 RNA screener, with a given set of  
 parameters (Figures 1D and S2). In order to understand why  
 the other sequences do not fold into G4s *in vitro*, the minimal  
 free energies (MFE) of the DNA and RNA sequences were  
 predicted using RNAfold.<sup>16</sup> All the SNPs had predicted MFEs  
 that were similar to that of the WT, specifically  $-13$  kcal/mol  
 for the RNA and  $-6$  to  $-7$  kcal/mol for the DNA sequences  
 (Figure S3). The absence of G4s in most structures can be  
 expected since two G-tetrad sequences are usually less stable  
 than the predicted Watson-Crick structures.<sup>17-19</sup> These  
 results make the  $\alpha$ -synuclein gene an ideal candidate with  
 which to evaluate the ability of different ligands to fold the

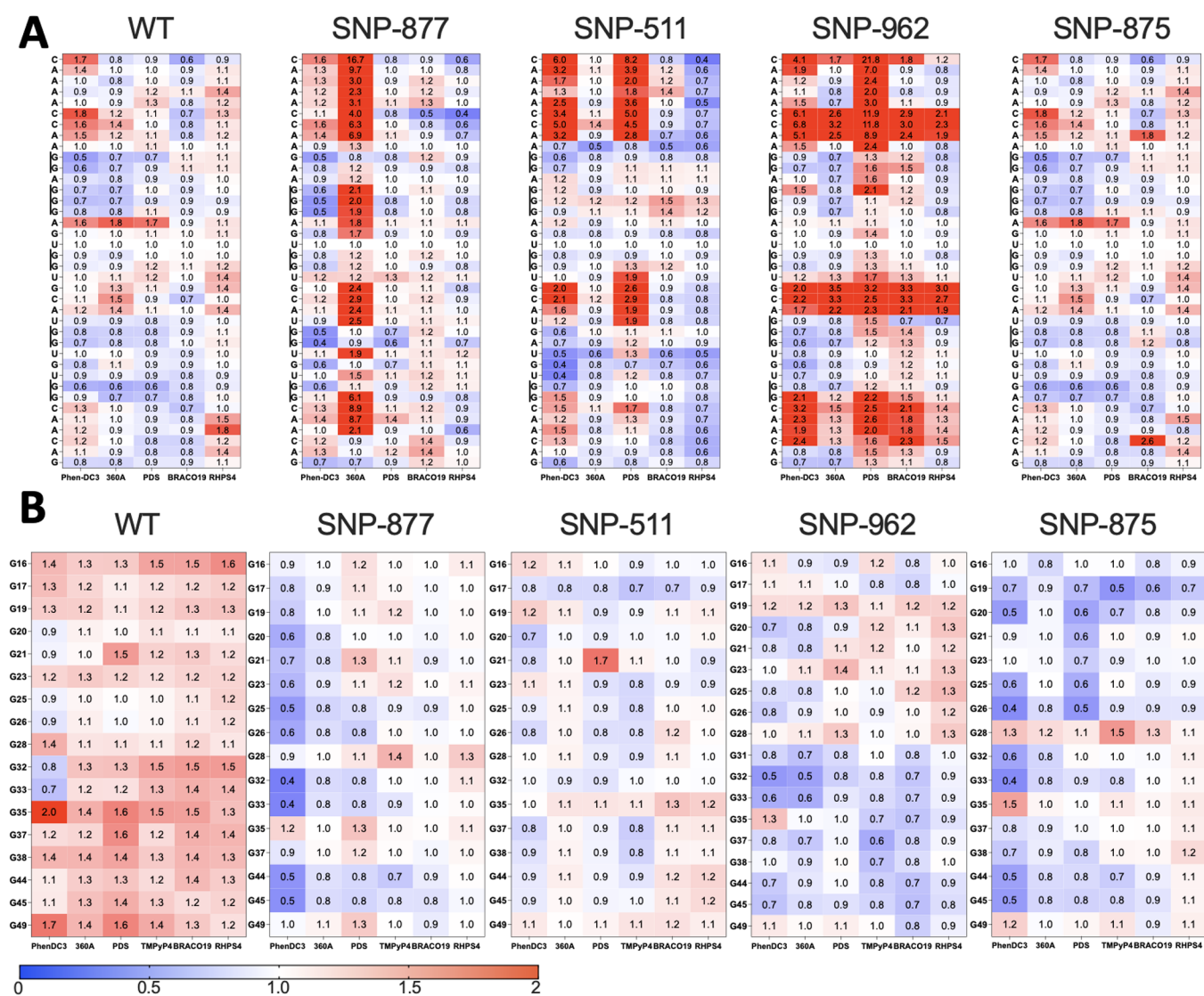


**Figure 2.** Single-nucleotide accessibility of the RNA and DNA sequences incubated with G4 ligands. (A) Heat maps illustrating the single-nucleotide accessibilities of the WT and the SNP sequences in *in-line* probing experiments in the presence of the different ligands. All nucleotides are shown. (B) Heat maps of the WT and the SNP sequences DMS footprinting experiments performed in the presence of the different ligands. The guanines are shown. For both experiments, the peaks were quantified by densitometry and then normalized to the KCl condition. The legend shows the fold change color palette over the KCl condition.

109 SNP sequences into G4s since most sequence variants do not  
110 seem to fold into G4 structures in both DNA and RNA.

111 In order to evaluate the impact of the ligands on the  
112 secondary structure, the accessibility of individual nucleotides  
113 to each sequence incubated with G4 ligands was monitored.  
114 This was done by either *in-line* probing for RNA (Figure 1A)  
115 or by dimethyl sulfate (DMS) footprinting for DNA (Figure  
116 1B), respectively. *In-line* probing is based on spontaneous  
117 hydrolysis of RNA in the presence of a high concentration of  
118 magnesium, while DMS footprinting is based on guanine  
119 nitrogen 7 (N7) methylation and piperidine strand break.<sup>20,21</sup>

120 In the *in-line* probing, the nucleotide located in a duplex or the  
121 G4 core should be protected from cleavage, in opposition to  
122 the ones located in the loops or flanking the G4. In the case of  
123 DMS footprinting, the guanines implicated in a Hoogsteen  
124 base pairing (e.g., in the G4 core) are expected to be less  
125 cleaved than the one in the loops or in the flanking sequences.  
126 The reactions were analyzed by electrophoresis on denaturing  
127 polyacrylamide gels, then were quantified by densitometry

(Figures S4 and S5) and the results normalized to the KCl  
128 condition (Figure 2). The experiments have been performed  
129 with three families of ligands: pyridodicarboxamide (Phen-  
130 DC3, 360A and PDS) and acridine (BRACO19 and  
131 RHPS4).<sup>3,22–24</sup> These ligands were selected because of their  
132 high selectivity for G4 and their popularity within the G4  
133 research community.<sup>3</sup> Additionally, these ligands have been  
134 reported to both stabilize and induce the formation of G4  
135 structures within two G-quartet motifs in long noncoding  
136 RNA.<sup>25</sup> The popular porphyrin TMPyP4 was also added into  
137 the analysis, even though some suggest that it could be also a  
138 G4 destabilizing ligand.<sup>26,27</sup> These two methods showed  
139 nucleotide accessibility modifications depending on both the  
140 ligands and the SNPs used. Global changes were also noticed  
141 between RNA and DNA accessibilities depending on the  
142 ligand used. For the RNA sequences, in SNP-962 (U > G), the  
143 nucleotides located upstream of the first stretch of guanines,  
144 those located between the third and the fourth stretches of  
145 guanines, and those located downstream of the last stretch of 146

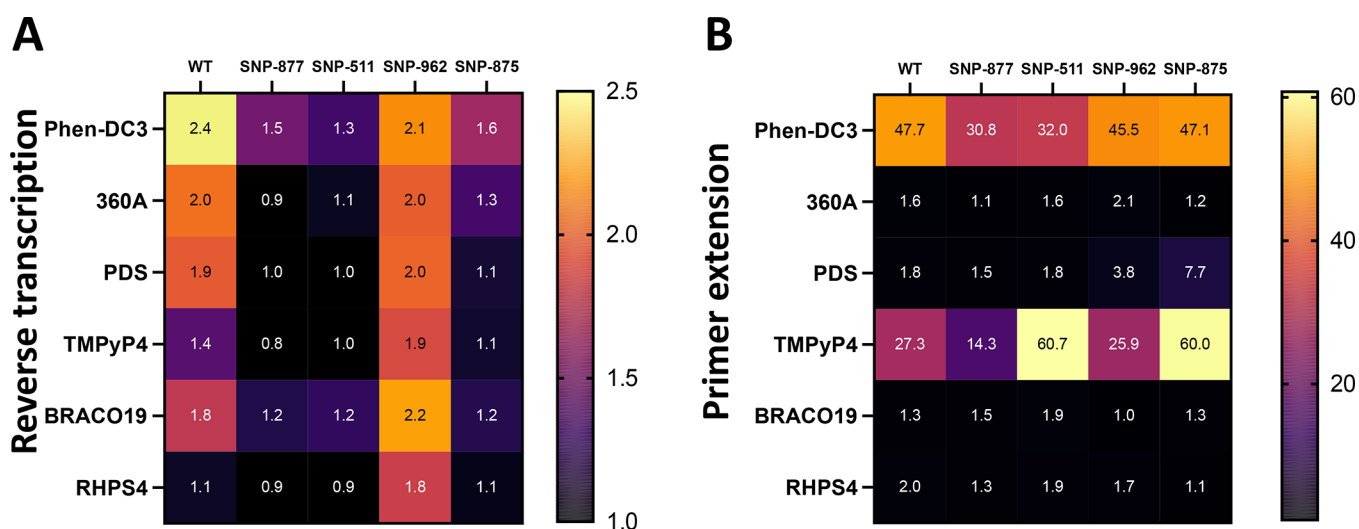


**Figure 3.** Evaluation of the stalling sites induced by the ligands. Data were plotted as heat plots. (A) Results from the RTS assays in the presence of 10 equiv of the ligands. The stalling sites were quantified for each ligand, and then were normalized to the KCl condition. (B) Results from the PE assays in the presence of 9 equiv of the ligands. The stalling sites were quantified for each ligand and then were normalized to the KCl condition. The legend shows the fold change color palette over the KCl condition. Together, the results presented in this Letter show that the SNPs present in  $\alpha$ -synuclein have a strong impact on G4 ligand response. Three SNPs were shown to reduce this response, and one was shown to be beneficial for G4 folding and to inhibit polymerase progression. Although the G4 ligands are quite similar chemically (i.e., they are rich in planar, aromatic cyclic moieties), the observed differences in stabilization efficiencies have been well documented over the past 20 years.<sup>5</sup> However, their differential impacts on SNPs, especially on RNA G4s, are very clear here. To our knowledge, this is the first report describing the effect of SNPs on G4 ligand binding efficacy and specificity. While this study used  $\alpha$ -synuclein as a proof-of-concept, SNPs are highly prevalent in the human genome and the interception of those with G4s must be considered for future G4 targeting. This concept is of importance for personalized medicine, where a weaker ligand could be selected to stabilize a desired SNP-G4 patient, without stabilizing every G4 and deregulating signaling pathways in cells.

147 guanines become, in general, at least 2 times more accessible to  
 148 all ligands. This is characteristic of G4s.<sup>20</sup> The accessibility in  
 149 SNP-511 seems to be highly modified only when it is  
 150 incubated with both Phen-DC3 and 360A, where a 6- to 8-  
 151 fold change was observed. All other ligands were observed to  
 152 have a mild effect. Most of the SNP-511 structure is less  
 153 accessible when incubated with RHPS4, a phenomenon  
 154 observed only for this candidate. One possible way of  
 155 explaining this observation is that a different type of G4 is  
 156 folded in the presence of RHPS4. BRACO19 is the only ligand  
 157 that induces a modification in base accessibility for SNP-875,  
 158 while 360A is the only one that does so for SNP-877, ranging  
 159 from 2- to 3- and 2- to 16-fold, respectively. The accessibilities  
 160 of the WT and SNP-875 are less affected than those of the  
 161 other three SNPs. In the case of the DNA sequences, the WT  
 162 guanine accessibilities seem to increase with the presence of  
 163 the ligands, up to a maximum change of 2-fold, except for  
 164 Phen-DC3 where a mixture of accessibility changes was  
 165 observed. The guanines in SNP-877, SNP-926, and SNP-875  
 166 were all around 2-fold less accessible when incubated with  
 167 Phen-DC3 as compared to those with the other ligands. Again,  
 168 this decrease is characteristic of G4 formation. PDS seems to  
 169 only be able to stabilize SNP-875. All ligands produced a clear  
 170 cleavage pattern in *in-line* probing experiments (Figure S4),  
 171 except for TMPyP4 where a smear was observed. Con-  
 172 sequently, it is hard to conclude and be quantitative in the case  
 173 of TMPyP4. TMPyP4 has been described as a promising G4  
 174 ligand in many studies, but recently, doubts have been raised  
 175 about its efficacy.<sup>28</sup> Dynamic light scattering experiments have  
 176 revealed that the G4 stabilization/destabilization capacity of  
 177 TMPyP4 is often misinterpreted because of its capacity to  
 178 induce precipitation. The smear results mentioned above could  
 179 confirm the occurrence of precipitation.<sup>28</sup> Globally, these

results show that, depending on the SNP, the ligands induced  
 differential folding on the different nucleic acid sequences.

Next, it was attempted to see if these nucleotide accessibility  
 differences would lead to a difference in polymerase  
 progression through the newly folded structure. With this  
 aim, the sequences were incubated with the ligands and then  
 were analyzed by a reverse transcriptase stalling assay (RTS)  
 for RNA and by primer extension (PE) assay for DNA. For  
 both techniques, a hairpin was added at the end of each  
 sequence for primer hybridization, as described previously.<sup>29</sup>  
 Importantly, these hairpins were not able to induce, nor able to  
 impair, the natural structure of the  $\alpha$ -synuclein sequences  
 (Figures S6 and S7). All of the reactions were analyzed by  
 electrophoresis on denaturing polyacrylamide gels and then  
 were quantified by densitometry (Figures S8 and S9). The  
 stalling assays were initially performed in the presence of either  
 LiCl or KCl without any ligands to see if G4s could naturally  
 impact the enzyme's progression (Figures S8 and S9, lanes 2  
 and 3). These results showed a differential response to the  
 cation used in both RTS and PE, with the LiCl condition  
 showing slightly more stalling sites than did the KCl one.  
 These differential efficiencies of the enzyme's progression  
 between LiCl and KCl were not expected, since G4s are  
 generally considered to be absent in the presence of LiCl and  
 would therefore not induce any more. Thus, the processivity of  
 the enzyme seems to be affected by the cation used. Even  
 though SNP-962 RNA was shown to fold into a G4 by  
 fluorescence assay (Figure 1), the structure formed in the  
 presence of KCl is not stable enough to induce stalling (Figure  
 S8, see SNP-962 in lane 3). Subsequently, the RTS and PE  
 were performed in the presence of 9 to 10 equiv of ligand in  
 the presence of KCl in order to both promote G4 folding and  
 to mimic intracellular conditions.<sup>30</sup> Data were normalized to 212

213 the KCl condition so as to accommodate for cation  
214 processivity. For the RTS assays, both the WT and the SNP-  
215 962 RNA sequences, when incubated with the ligands, were  
216 shown to induce more stalling sites than did the three other  
217 SNPs (except for the WT in the presence of RHPS4; Figure  
218 3A). These two candidates were the ones with the highest G4  
219 scores. Therefore, all guanine doublets seem to be of some  
220 importance for ligand stabilization, and the conversion of a  
221 doublet into a triplet highly increases the response. Based on  
222 both the fluorescent and the RTS results, the absence of a  
223 signal with the NMM ligands and the strong stalling site for the  
224 WT points toward the presence of new ligand-induced G4s,  
225 while ligand-stabilizing effects are most likely what happened  
226 in the case of SNP-962, as evidenced by the initial fluorescence  
227 observed with NMM and by the strong stalling site. The Phen-  
228 DC3 ligand was able to induce stalling sites when incubated  
229 with each RNA candidate. This had previously been  
230 demonstrated, more specifically that Phen-DC3 acts as a  
231 chaperone for RNA G4 folding with long-non coding RNA.<sup>25</sup>  
232 Of note, two weak stalling sites that are not located in front of  
233 any stretch of guanines seem to be present in each  
234 construction with BRACO19, i.e., at positions 58 and 59.  
235 This could be attributed to the nonspecific binding interaction  
236 of BRACO19, previously reported with duplex and triplex  
237 structures.<sup>31</sup> For the PE assays, the stop differences between  
238 the KCl condition and the best ligands (Phen-DC3 and  
239 TMPyP4) were much stronger (on average around 40-fold  
240 versus 2-fold). Of note, while the PE assays were performed  
241 with Taq polymerase at 37 °C, the RTS assays were performed  
242 with reverse transcriptase (MMuLV) at 45 °C, which can have  
243 the effect of reducing G4 propensity as compared to what is  
244 seen at 37 °C. This could explain the stalling difference  
245 between the two experiments. Phen-DC3 was also found to be  
246 highly efficient in increasing the number of stalling sites of each  
247 DNA candidate. A reduction in the complete TMPyP4 product  
248 was also noted. However, as was observed in the *in-line*  
249 experiments, it seems like TMPyP4 induced precipitation since  
250 no apparent stop can be identified prior to the final one (as  
251 seen previously<sup>28</sup>). Contrary to the RTS results, DNA WT and  
252 SNP-962 did not seem to inhibit the polymerase's progression  
253 at the same level with each ligand. A particular polymerase-  
254 impairing interaction between SNP-875 and PDS seems to be  
255 specific for this pair (7.7-fold). Once again, these results point  
256 toward a differential binding of the ligands for the different  
257 sequences and a different response between DNA and RNA  
258 G4s to the ligands.

## 259 ■ ASSOCIATED CONTENT

### 260 ■ Supporting Information

261 The Supporting Information is available free of charge at  
262 <https://pubs.acs.org/doi/10.1021/acschembio.4c00104>.

263 Material and Methods and additional experimental  
264 figures and tables; G4RNA Screener scores by position;  
265 NMM fluorescence; structure prediction; gel analysis  
266 (PDF)

267 QGRS analysis (XLSX)

268 Oligonucleotides used in this study (XLSX)

## 269 ■ AUTHOR INFORMATION

### 270 Corresponding Author

271 Jean-Pierre Perreault – Department of Biochemistry and  
272 Functional Genomics, Pavillon de Recherche Appliquée sur le

Cancer, Université de Sherbrooke, Sherbrooke, Québec J1E  
4K8, Canada; [orcid.org/0000-0002-4559-5541](https://orcid.org/0000-0002-4559-5541);  
Phone: 819-821-8283; Email: [jean-pierre.perreault@usherbrooke.ca](mailto:jean-pierre.perreault@usherbrooke.ca); Fax: 819-564-5340

### 273 Author

Marc-Antoine Turcotte – Department of Biochemistry and  
Functional Genomics, Pavillon de Recherche Appliquée sur le  
Cancer, Université de Sherbrooke, Sherbrooke, Québec J1E  
4K8, Canada

274 Complete contact information is available at:

<https://pubs.acs.org/10.1021/acschembio.4c00104>

### 275 Author Contributions

M.A.T. and J.P.P. conceptualized this study. M.A.T. performed  
the experiments. M.A.T. and J.P.P. analyzed the data. MAT  
and JPP wrote and revised the manuscript.

### 276 Funding

This project was supported by grants from the Natural  
Sciences and Engineering Research Council of Canada  
(NSERC; RGPIN-2023-04178 to J.P.P.). M.A.T. received  
student fellowships from the Fonds de Recherche Québec  
Nature et Technologie (FRQNT) and the Canadian Institutes  
of Health Research (CIHR). J.P.P. holds the Research Chair of  
the Université de Sherbrooke in RNA Structure and Genomics  
and is a member of the Centre de Recherche du CHUS. The  
funders had no role in study design, data collection and  
analysis, the decision to publish, or in the preparation of the  
manuscript.

### 277 Notes

The authors declare no competing financial interest.

## 278 ■ ACKNOWLEDGMENTS

We thank P. Lejault for 360A synthesis as well as for critical  
reading of the initial manuscript.

## 279 ■ REFERENCES

- (1) Varshney, D.; Spiegel, J.; Zyner, K.; Tannahill, D.; Balasubramanian, S. The Regulation and Functions of DNA and RNA G-Quadruplexes. *Nat. Rev. Mol. Cell Biol.* **2020**, *21*, 459–474.
- (2) Rhodes, D.; Lipps, H. J. G-Quadruplexes and Their Regulatory Roles in Biology. *Nucleic Acids Res.* **2015**, *43* (18), 8627–8637.
- (3) Wang, Y.-H.; Yang, Q.-F.; Lin, X.; Chen, D.; Wang, Z.-Y.; Chen, B.; Han, H.-Y.; Chen, H.-D.; Cai, K.-C.; Li, Q.; Yang, S.; Tang, Y.-L.; Li, F. G4LDB 2.2: A Database for Discovering and Studying G-Quadruplex and i-Motif Ligands. *Nucleic Acids Res.* **2022**, *50* (D1), D150–D160.
- (4) Le, D. D.; Di Antonio, M.; Chan, L. K. M.; Balasubramanian, S. G-Quadruplex Ligands Exhibit Differential G-Tetrad Selectivity. *Chem. Commun.* **2015**, *51* (38), 8048–8050.
- (5) Zhang, S.; Wu, Y.; Zhang, W. G-Quadruplex Structures and Their Interaction Diversity with Ligands. *ChemMedChem.* **2014**, *9* (5), 899–911.
- (6) Švehlová, K.; Lawrence, M. S.; Bednářová, L.; Curtis, E. A. Altered Biochemical Specificity of G-Quadruplexes with Mutated Tetrads. *Nucleic Acids Res.* **2016**, *44* (22), 10789–10803.
- (7) Nassar, L. R.; Barber, G. P.; Benet-Pagès, A.; Casper, J.; Clawson, H.; Diekhans, M.; Fischer, C.; Gonzalez, J. N.; Hinrichs, A. S.; Lee, B. T.; Lee, C. M.; Muthuraman, P.; Nguy, B.; Pereira, T.; Nejad, P.; Perez, G.; Raney, B. J.; Schmelter, D.; Speir, M. L.; Wick, B. D.; Zweig, A. S.; Haussler, D.; Kuhn, R. M.; Haeussler, M.; Kent, W. J. The UCSC Genome Browser Database: 2023 Update. *Nucleic Acids Res.* **2023**, *51* (D1), D1188–D1195.
- (8) Gong, J.; Wen, C.; Tang, M.; Duan, R.; Chen, J.; Zhang, J.; Zheng, K.; He, Y.; Hao, Y.; Yu, Q.; Ren, S.; Tan, Z. G-Quadruplex

- 334 Structural Variations in Human Genome Associated with Single-  
335 Nucleotide Variations and Their Impact on Gene Activity. *Proc. Natl.*  
336 *Acad. Sci. U. S. A.* **2021**, *118* (21), No. e2013230118.
- 337 (9) Li, Y.; He, Z.; Li, Z.; Lu, Y.; Xun, Q.; Xiang, L.; Zhang, M. G-  
338 Quadruplex Formation within the Promoter Region of HSPB2 and Its  
339 Effect on Transcription. *Heliyon* **2024**, *10* (2), No. e24396.
- 340 (10) Mehra, S.; Sahay, S.; Maji, S. K.  $\alpha$ -Synuclein Misfolding and  
341 Aggregation: Implications in Parkinson's Disease Pathogenesis.  
342 *Biochimica et Biophysica Acta (BBA) - Proteins and Proteomics* **2019**,  
343 *1867* (10), 890–908.
- 344 (11) Garant, J.-M.; Perreault, J.-P.; Scott, M. S. G4RNA Screener  
345 Web Server: User Focused Interface for RNA G-Quadruplex  
346 Prediction. *Biochimie* **2018**, *151*, 115–118.
- 347 (12) Bedrat, A.; Lacroix, L.; Mergny, J.-L. Re-Evaluation of G-  
348 Quadruplex Propensity with G4Hunter. *Nucleic Acids Res.* **2016**, *44*  
349 (4), 1746–1759.
- 350 (13) Beaudoin, J.-D.; Jodoin, R.; Perreault, J.-P. New Scoring System  
351 to Identify RNA G-Quadruplex Folding. *Nucleic Acids Res.* **2014**, *42*  
352 (2), 1209–1223.
- 353 (14) Kikin, O.; D'Antonio, L.; Bagga, P. S. QGRS Mapper: A Web-  
354 Based Server for Predicting G-Quadruplexes in Nucleotide Sequences.  
355 *Nucleic Acids Res.* **2006**, *34* (Web Server), W676–W682.
- 356 (15) Nicoludis, J. M.; Barrett, S. P.; Mergny, J.-L.; Yatsunyk, L. A.  
357 Interaction of Human Telomeric DNA with N-Methyl Mesopor-  
358 phyrin IX. *Nucleic Acids Res.* **2012**, *40* (12), 5432–5447.
- 359 (16) Lorenz, R.; Bernhart, S. H.; Höner zu Siederdisen, C.; Tafer,  
360 H.; Flamm, C.; Stadler, P. F.; Hofacker, I. L. ViennaRNA Package 2.0.  
361 *Algorithms Mol. Biol.* **2011**, *6*, 26.
- 362 (17) Jana, J.; Weisz, K. Thermodynamic Stability of G-Quad-  
363 ruplexes: Impact of Sequence and Environment. *Chembiochem* **2021**,  
364 *22* (19), 2848–2856.
- 365 (18) Lorenz, R.; Bernhart, S. H.; Externbrink, F.; Qin, J.; Höner zu  
366 Siederdisen, C.; Amman, F.; Hofacker, I. L.; Stadler, P. F. RNA  
367 Folding Algorithms with G-Quadruplexes. In *Advances in Bioinform-*  
368 *matics and Computational Biology*; Springer: Berlin, 2012; pp 49–60.  
369 DOI: [10.1007/978-3-642-31927-3\\_5](https://doi.org/10.1007/978-3-642-31927-3_5).
- 370 (19) Zhang, A. Y. Q.; Balasubramanian, S. The Kinetics and Folding  
371 Pathways of Intramolecular G-Quadruplex Nucleic Acids. *J. Am.*  
372 *Chem. Soc.* **2012**, *134* (46), 19297–19308.
- 373 (20) Beaudoin, J.-D.; Jodoin, R.; Perreault, J.-P. In-Line Probing of  
374 RNA G-Quadruplexes. *Methods* **2013**, *64* (1), 79–87.
- 375 (21) Tijerina, P.; Mohr, S.; Russell, R. DMS Footprinting of  
376 Structured RNAs and RNA-Protein Complexes. *Nat. Protoc* **2007**, *2*  
377 (10), 2608–2623.
- 378 (22) Granotier, C.; Pennarun, G.; Riou, L.; Hoffschir, F.; Gauthier,  
379 L. R.; De Cian, A.; Gomez, D.; Mandine, E.; Riou, J.-F.; Mergny, J.-L.;  
380 Mailliet, P.; Dutrillaux, B.; Boussin, F. D. Preferential Binding of a G-  
381 Quadruplex Ligand to Human Chromosome Ends. *Nucleic Acids Res.*  
382 **2005**, *33* (13), 4182–4190.
- 383 (23) Moore, M. J. B.; Schultes, C. M.; Cuesta, J.; Cuenca, F.;  
384 Gunaratnam, M.; Tanius, F. A.; Wilson, W. D.; Neidle, S.  
385 Trisubstituted Acridines as G-Quadruplex Telomere Targeting  
386 Agents. Effects of Extensions of the 3,6- and 9-Side Chains on  
387 Quadruplex Binding, Telomerase Activity, and Cell Proliferation. *J.*  
388 *Med. Chem.* **2006**, *49* (2), 582–599.
- 389 (24) Gowan, S. M.; Heald, R.; Stevens, M. F.; Kelland, L. R. Potent  
390 Inhibition of Telomerase by Small-Molecule Pentacyclic Acridines  
391 Capable of Interacting with G-Quadruplexes. *Mol. Pharmacol.* **2001**,  
392 *60* (5), 981–988.
- 393 (25) Lejault, P.; Prudent, L.; Terrier, M.-P.; Perreault, J.-P. Small  
394 Molecule Chaperones Facilitate the Folding of RNA G-Quadruplexes.  
395 *Biochimie* **2023**, *214*, 83–90.
- 396 (26) Han, F. X.; Wheelhouse, R. T.; Hurley, L. H. Interactions of  
397 TMPyP4 and TMPyP2 with Quadruplex DNA. Structural Basis for  
398 the Differential Effects on Telomerase Inhibition. *J. Am. Chem. Soc.*  
399 **1999**, *121* (15), 3561–3570.
- 400 (27) Weisman-Shomer, P.; Cohen, E.; Hershco, I.; Khateb, S.;  
401 Wolfowitz-Barchad, O.; Hurley, L. H.; Fry, M. The Cationic Porphyrin  
402 TMPyP4 Destabilizes the Tetraplex Form of the Fragile X Syndrome  
Expanded Sequence d(CGG)<sub>n</sub>. *Nucleic Acids Res.* **2003**, *31* (14), 403  
3963–3970. 404
- (28) Mitteau, J.; Lejault, P.; Wojciechowski, F.; Joubert, A.; 405  
Boudon, J.; Desbois, N.; Gros, C. P.; Hudson, R. H. E.; Boulé, J.-B.; 406  
Granzhan, A.; Monchaud, D. Identifying G-Quadruplex-DNA- 407  
Disrupting Small Molecules. *J. Am. Chem. Soc.* **2021**, *143* (32), 408  
12567–12577. 409
- (29) Lyu, K.; Kwok, C. K. RNA G-Quadruplex (rG4) Structure 410  
Detection Using RTS and SHALiPE Assays. *Methods Enzymol* **2023**, 411  
*691*, 63–80. 412
- (30) Zacchia, M.; Abategiovanni, M. L.; Stratigis, S.; Capasso, G. 413  
Potassium: From Physiology to Clinical Implications. *Kidney Dis* 414  
(Basel) **2016**, *2* (2), 72–79. 415
- (31) Tran, P. L. T.; Largy, E.; Hamon, F.; Teulade-Fichou, M.-P.; 416  
Mergny, J.-L. Fluorescence Intercalator Displacement Assay for 417  
Screening G4 Ligands towards a Variety of G-Quadruplex Structures. 418  
*Biochimie* **2011**, *93* (8), 1288–1296. 419